

## Translaminar fracture toughness of discontinuous, aligned flax fibre composites

C. Canturri<sup>1</sup>, L.Q.N. Tran<sup>2</sup>, C.L.C. Tan<sup>3</sup> and W.S. Teo<sup>4</sup>

<sup>1</sup> Email: [carla\\_canturri@simtech.a-star.edu.sg](mailto:carla_canturri@simtech.a-star.edu.sg) Singapore Institute of Manufacturing Technology, Agency for Science, Technology and Research (A\*STAR), Fusionopolis Way, Innovis Tower, 138634, Singapore

<sup>2</sup> Email: [tranlqn@simtech.a-star.edu.sg](mailto:tranlqn@simtech.a-star.edu.sg) Singapore Institute of Manufacturing Technology, Agency for Science, Technology and Research (A\*STAR), Fusionopolis Way, Innovis Tower, 138634, Singapore

<sup>3</sup> Email: [clara-tan@simtech.a-star.edu.sg](mailto:clara-tan@simtech.a-star.edu.sg) Singapore Institute of Manufacturing Technology, Agency for Science, Technology and Research (A\*STAR), Fusionopolis Way, Innovis Tower, 138634, Singapore

<sup>4</sup> Email: [wsteo@simtech.a-star.edu.sg](mailto:wsteo@simtech.a-star.edu.sg) Singapore Institute of Manufacturing Technology, Agency for Science, Technology and Research (A\*STAR), Fusionopolis Way, Innovis Tower, 138634, Singapore

**Keywords:** flax, strain energy release ( $G_c$ ), discontinuous fibre, flax-epoxy prepreg, translaminar

### Abstract

This paper describes the results of an investigation into Mode I translaminar critical strain energy release rate of continuous laminates and slit-cut laminates. The aims of the work were to define the fracture properties of flax-epoxy prepreg laminates for component design and to investigate the active fracture mechanisms. Compact tension tests were performed using cross ply unidirectional laminates, one with continuous 0° plies and one with slit cuts in the 0° plies. The behaviour of the material observed during the test revealed a lower initiation critical energy release rate for the discontinuous laminates. The R-curve was only established for the discontinuous laminates and showed a rising behaviour due to bridging of the interfaces. It was found that different fracture mechanisms acted in the two laminates, single fibre pull-out was observed in the continuous laminates and bundle pull-out was observed in the discontinuous laminates.

### 1. Introduction

In the past ten years, the composite industry has seen an increase in the usage of flax fibre composites to replace glass fibre composites. Flax fibres have similar stiffness than glass fibres, are tough and exhibit the highest strength among other bast fibres [1]. Flax fibre composites have found applications in the automotive industry as reinforcement for panels with enhanced acoustic properties and also as structural elements in bike frames, helmets and other sporting equipment. If flax fibre composites are to be used with confidence for such semi-structural applications it will require the characterisation of static and dynamic properties. One of the load cases to which such components are subjected is low-speed impact. It is recognised that the main failure mode of flax fibre-epoxy laminates in low-speed impact is translaminar failure with minimal delamination [2] due to the high interlaminar fracture toughness exhibited by flax-epoxy composites [3]. It is then important to characterise and quantify the translaminar critical strain energy release rate to determine the extent and severity of impact loads.

At the same time it has been studied by Bullegas et al. [4] that an increase of crack path deflection induced by a pattern of micro-cuts can be key for damage tolerant aerostructures of carbon fibre composite specimens while keeping similar un-notched tensile strengths. The patterns of the micro-cuts

are of hierarchical nature, and carefully designed, machined and placed to induce maximum fracture surfaces while minimising crack length growth.

Natural fibres exhibit an intrinsically discontinuous structure: a bast fibre is a composite of thinner and shorter elementary fibres bonded by pectin and hemicellulose. Despite this hierarchical structure that could suggest that relatively high toughness values can be achieved, past research showed that natural fibre composites can exhibit values of translaminar critical strain energy release rate of up to five times lower than glass fibre composites [5]. In an attempt to reduce the gap between synthetic and natural fibre composites, translaminar critical strain energy release rate could be improved by the use of discontinuous aligned fibre laminates. An increase in the crack tortuosity and thus higher fracture surface creation is expected. The low cost nature of these composites do not justify an advanced patterning method as suggested by Bullegas et al. [4] and an alternative method is explored in this paper inspired by other prepreg slit cut methods such as ACG's Deformable Composite System (DCS) [6]. Moreover this method opens the door to future usage of fibre preforms that have been designed to take advantage of the finite length of vegetal fibres. The use of discontinuous fibres, in opposition to continuously spun yarns, for natural fibre composites can also reduce production costs by eliminating the need for additional processing to obtain continuous yarns. Furthermore, less processed fibres are likely to present higher mechanical properties.

The aim of this project is to assess the translaminar critical strain energy release rate of aligned discontinuous flax fibre laminates relative to the translaminar critical strain energy release rate of continuous fibre laminates. A compact tension specimen configuration together with an FE-based compliance calibration data reduction method is used to measure the translaminar critical strain energy release rate of the two configurations. A stacking sequence of  $[(90/0)_4/90]_s$  is used with only the  $0^\circ$  ply containing discontinuities. The results obtained are benchmarked against the equivalent continuous fibre specimen. The crack path is studied by means of optical microscopy. Of a particular interest is the investigation of the hierarchical structure of flax fibres: the interaction of the translaminar crack and the technical/elementary fibres is analysed in post-mortem specimens to determine if the crack propagates through the pectin/hemicellulose binder or rather at the matrix/technical fibre interface.

## 2. Experimental details

Two panels were manufactured from Lineo FlaxPreg T-UD flax fibre-epoxy pre-preg  $110 \text{ g/m}^2$ . The panels were hand laid-up and press-cured at 15 bar for 1 h at  $140^\circ\text{C}$  with a layup of  $[(90/0)_4/90]_s$  to obtain 4 mm thick laminates. Two different configurations were studied to characterise the effect of fibre discontinuity. First, a purely UD laminate and second a laminate with discontinuous  $0^\circ$  plies. The discontinuities at the  $0^\circ$  plies were introduced with a perforating rotary cutter which produced 2.6 mm slits separated by 1 mm in rows separated by 5 mm. Although the overlap of the slits was difficult to control due to the manual nature of the process, care was taken to shift the slits in each row so as not to produce fibres longer than 10 mm as shown in Figure 1. The discontinuities were applied throughout the ply and in each  $0^\circ$  ply. Compact tension specimens were manufactured according to the dimensions used by Laffan et al [7] and reproduced in Figure 2a. Ten specimens were dry cut from the panels and a  $a_0=19 \text{ mm}$  long pre-crack was introduced with a 0.2 mm diamond coated wire saw to produce a sharp starter crack (Figure 2b). Specimens were pre dried in a  $70^\circ\text{C}$  oven for 24 h prior testing at room temperature. The specimens were tested in an Instron 5982 Universal Testing machine in displacement control at a stroke of 0.5 mm/min.

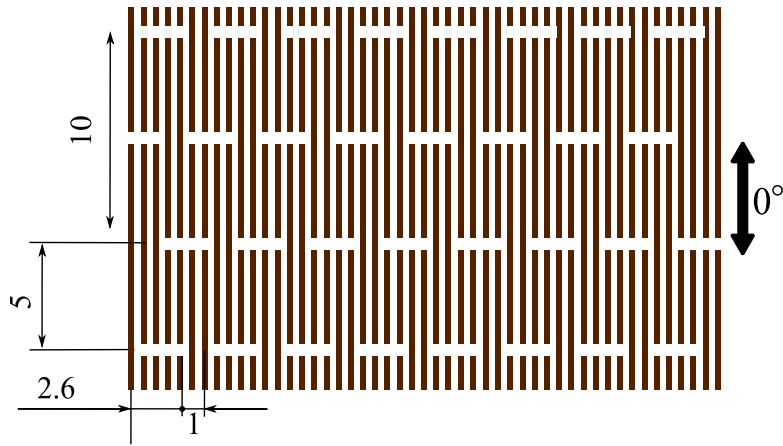


**Figure 1** Geometry of the slits introduced with rotary cutter tool.

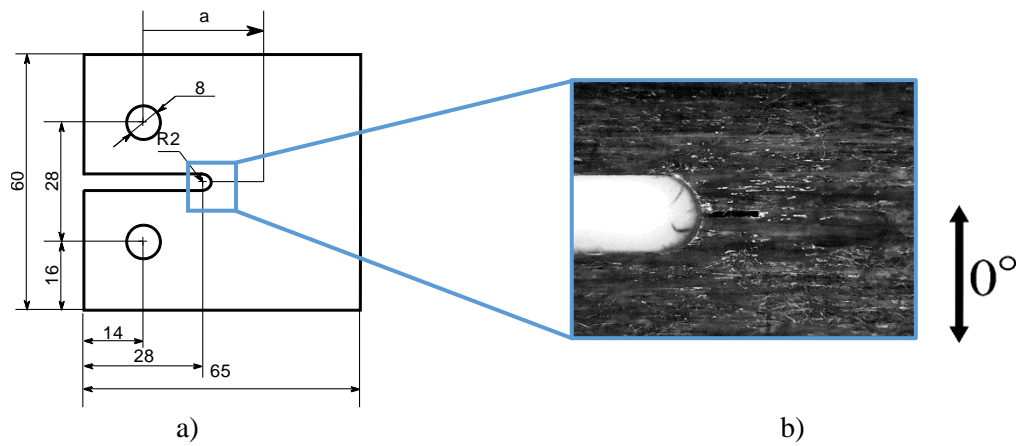


**Figure 2** a) Compact tension specimen dimensions from Laffan et al. [7] and b) detail of pre-crack obtained with wire saw.

### 3. Numerical data reduction

The numerically-based compliance calibration method for compact tension specimens as used by Laffan et al. and Ortega et al. [7], [8] was implemented to obtain the effective crack length without the need of optically monitoring the crack growth. The strain energy rate at which crack growth is observed is defined by the rate of change of compliance ( $C$ ) as the crack ( $a$ ) grows:

$$G_c = \frac{P^2}{2t} \frac{dC}{da} \quad (1)$$

Being  $P$  and  $t$ , the load and thickness, respectively. In this study, the compliance vs. crack length curve was obtained numerically. The compliance as a function of crack length was approximated by a 3rd order polynomial with coefficients  $\alpha$ ,  $\beta$ ,  $\gamma$  and  $\delta$ . To quantify the crack length the measure of  $a_{eff}$  is hereafter used as this is the calculated crack.

$$C = \alpha a_{eff}^3 + \beta a_{eff}^2 + \gamma a_{eff} + \delta \quad (2)$$

Combining Eq. 1 and Eq.2 we obtain:

$$G_c = \frac{P^2}{2t} (3\alpha a_{eff}^2 + 2\beta a_{eff} + \gamma) \quad (3)$$

It is necessary then to evaluate the effective crack length  $a_{eff}$  which can be found from the compliance vs. displacement experimental results and solving for  $a$  in Eq. 2.

The compliance vs. crack length curve was obtained with an FE model that simulated the specimen with a growing crack at fixed intervals of 1 mm from  $a_0=19$  mm to  $a_0=40$  mm. Half of the specimen was modelled with in Abaqus with 0.5 mm S8R5 shell elements. The boundary conditions were introduced as prescribed displacement in the node corresponding to the center of the pin and symmetry conditions at the symmetry axis. Nodes were released from the symmetry condition to simulate the crack growth.

## 4. Results

### 4.1 Experimental results

From the specimens initially manufactured, one discontinuous and one continuous were discarded due to drilling damage and oil ingress. Load initiation values were calculated at the first load drop or at a 5% loss of linearity, whichever occurred first. Compliance results were normalised by the thickness of the specimen. It can be seen in the load-displacement curve for a typical continuous plies and a typical discontinuous plies specimen shown in Figure 3 that the discontinuous plies laminate exhibited a marked stick-slip crack growth. The continuous laminate showed a more progressive growth with a minor stick-slip behaviour on the beginning of the propagation. Hence, propagation results were calculated only in the discontinuous laminates in the portions where the load increased after the crack had propagated. The summary of results is shown in Table 1. The few propagation values that could be obtained for the discontinuous laminates (as these showed a marked stick-slip crack growth) are presented in Figure 4. Note that the data correspond to different specimens and the values plotted are single points and not averaged across the specimens.

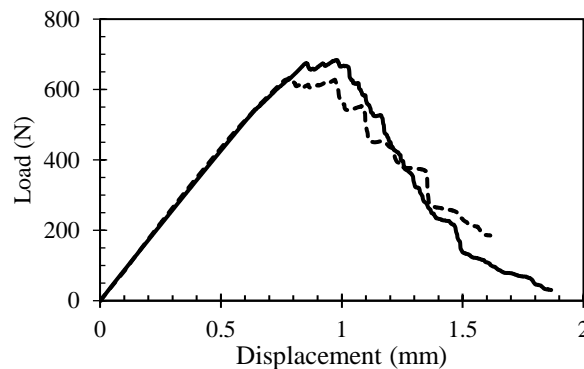


**Figure 3** Typical load-displacement curve for continuous compact tension specimen (continuous line) and specimen containing discontinuities (discontinuous line).

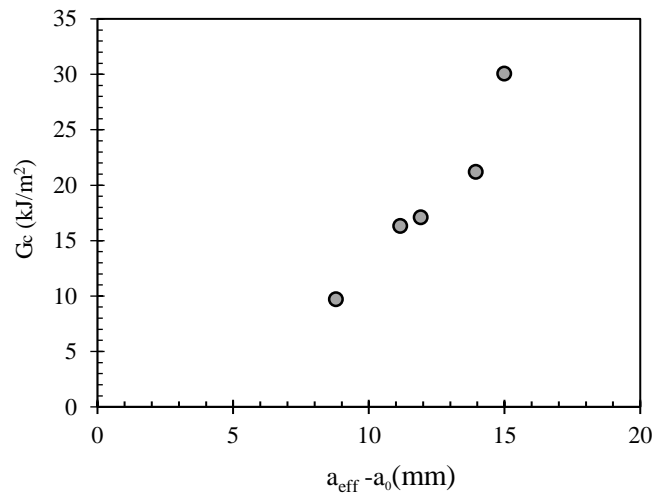


**Figure 4** R-curve of specimen containing discontinuities, across all specimens.

**Table 1.** Summary of tested specimens and results.

Specimen Type	Number of Valid Specimens	Initiation Load (N)	Initiation $G_c$ (kJ/m <sup>2</sup> )
Continuous	4	662.85 ± 11.66	10.18 ± 0.43
Discontinuous	4	615.99 ± 14.38	9.62 ± 1.21

The crack surfaces were exposed and the fractographic analysis was undertaken to glean the fracture mechanisms. An Olympus SZ61 stereomicroscope was used at magnifications between x1.25 and x4. The crack propagated in a single plane in the continuous laminate. In the case of the discontinuous laminates, the crack deviated from the original crack plane and propagated close to the discontinuities plane, resulting in different fracture planes per each 0° ply. Both specimens showed extensive pull-out on the 0° ply although of a different nature, single fibres and small fibre bundles pulled-out in the continuous laminate while for the case of discontinuous laminates it was whole fibre bundles. Shear cusps (Figure 5b) could be observed in the flanks of the pulled out bundles. Small fibre bundles were also pulled out from the continuous laminate as can be seen in Figure 5a.

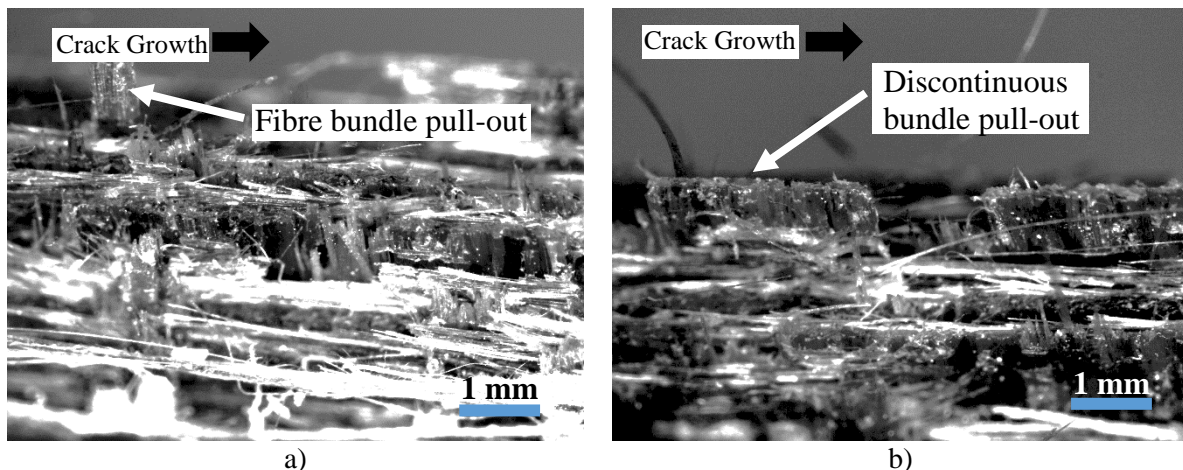


**Figure 5** Fracture surfaces of a) continuous laminate and b) discontinuous laminate.

## 5. Discussion

The performance of the discontinuous laminates in terms of initiation  $G_c$  was consistently lower than the continuous counterpart. Propagation values of the continuous laminates were not captured because of the progressive nature of the failure made it impossible to determine the compliance during the test as the crack propagated. The alternative of un-loading re-loading the specimen to measure the residual compliance could be evaluated but in material systems where fibre pull-out is significant the results would be altered by the presence of the pull-outs. The measurement of compliance was possible with the discontinuous specimens that showed a stick-slip type of crack growth. Although the data points generated were insufficient to effectively determine the R-curve, the upwards trend was significant and can be associated with the large degree of fibre bridging observed in the 90° plies. This would be in agreement with the large process zone and fibre bridging observed in interlaminar critical strain energy release rate test of UD flax systems.

Fractographically, the observation of shear cusps at the flanks of pulled-out bundles would be an indication of secondary failure modes interacting with the main translaminar crack and serving as energy dissipation mechanisms. However, this was not translated to an increase of initiation  $G_c$  and no data is available to compare propagation values for both configurations. Similarly, the crack deviated to propagate through the discontinuities without a noticeable effect in the initiation  $G_c$ . Further work will include different fibre length distribution and ratio to aim for an improvement of the  $G_c$ . Also, if the aim is solely to increase the critical strain energy release rate of the component, other strategies can be explored such as ply blocking as studied by Teixeira et al. [9]. Also, the effect of a thermoplastic matrix will be explored.

## 6. Conclusion

The effect of cut slits in a flax-epoxy prepreg on the translaminar  $G_c$  was investigated in this paper. The induced discontinuities were introduced with a rotary cutter tool and a compact tension specimen was used for the mechanical testing. Initiation critical strain energy release rates were determined for specimens containing discontinuities and for those with pristine fibres, these were  $9.62 \pm 1.21$  and  $10.18 \pm 0.43$  kJ/m<sup>2</sup>, respectively. However, due to the nature of the crack growth, propagation values could not be established for the laminates with continuous fibres. For those specimens showing a stick-slip crack growth behaviour, the propagation values of critical strain energy release rate could be determined and an increase of  $G_c$  as the crack propagated was observed. The main failure mechanism was fibre and bundle pull-out together with crack deviation for those specimens containing discontinuities.

## 7. References

- [1] L. Pil, F. Bensadoun, J. Pariset, and I. Verpoest, "Why are designers fascinated by flax and hemp fibre composites?," *Compos. Part A Appl. Sci. Manuf.*, vol. 83, pp. 193–205, 2016.
- [2] M. Ravandi, W. S. Teo, L. Q. N. Tran, M. S. Yong, and T. E. Tay, "Low velocity impact performance of stitched flax/epoxy composite laminates," *Compos. Part B Eng.*, vol. 117, pp. 89–100, May 2017.
- [3] M. Ravandi, W. S. Teo, L. Q. N. Tran, M. S. Yong, and T. E. Tay, "The effects of through-the-thickness stitching on the Mode I interlaminar fracture toughness of flax/epoxy composite laminates," *Mater. Des.*, vol. 109, pp. 659–669, Nov. 2016.
- [4] G. Bullegas, S. T. Pinho, and S. Pimenta, "Engineering the translaminar fracture behaviour of thin-ply composites," *Compos. Sci. Technol.*, vol. 131, pp. 110–122, Aug. 2016.

- [5] M. Hughes, C. A. S. Hill, and J. R. B. Hague, "The fracture toughness of bast fibre reinforced polyester composites Part 1 Evaluation and analysis," *J. Mater. Sci.*, vol. 37, no. 21, pp. 4669–4676, 2002.
- [6] J. Nixon, "The best of both worlds," *Reinf. Plast.*, vol. 52, no. 4, pp. 36–39, 2008.
- [7] M. J. Laffan, S. T. Pinho, P. Robinson, and L. Iannucci, "Measurement of the in situ ply fracture toughness associated with mode I fibre tensile failure in FRP. Part II: Size and lay-up effects," *Compos. Sci. Technol.*, vol. 70, no. 4, pp. 614–621, Apr. 2010.
- [8] A. Ortega, P. Maimí, E. V. González, and L. Ripoll, "Compact tension specimen for orthotropic materials," *Compos. Part A Appl. Sci. Manuf.*, vol. 63, pp. 85–93, Aug. 2014.
- [9] R. F. Teixeira, S. T. Pinho, and P. Robinson, "Thickness-dependence of the translaminar fracture toughness: Experimental study using thin-ply composites," *Compos. Part A Appl. Sci. Manuf.*, vol. 90, pp. 33–44, Nov. 2016.